Journal of Molecular Structure 1219 (2020) 128526

Contents lists available at ScienceDirect

Journal of Molecular Structure

journal homepage: http://www.elsevier.com/locate/molstruc

Two new Cu(II) and Ni(II) 1,10-phenanthroline complexes with anions of barbituric acids in the outer sphere: Synthesis, structure, spectroscopic, magnetic and thermal properties

Nicolay N. Golovnev [a], Maxim S. Molokeev [b, a, c, *], Irina V. Sterkhova [d], Maxim K. Lesnikov [a], Anastasia V. Demina [a], Gennady S. Patrin [e, a]

[a] Siberian Federal University, 79 Svobodny Ave., Krasnoyarsk, 660041, Russia
[b] Laboratory of Crystal Physics, Kirensky Institute of Physics, Federal Research Center KSC SB RAS, Bld. 38 Akademgorodok 50, Krasnoyarsk, 660036, Russia
[c] Department of Physics, Far Eastern State Transport University, 47 Seryshev Str., Khabarovsk, 680021, Russia
[d] Favorsky Institute of Chemistry, Siberian Branch, Russian Academy of Sciences, 1 Favorsky, Irkutsk, 664033, Russia
[e] Laboratory of Magnetic Dynamics, Kirensky Institute of Physics, Federal Research Center KSC SB RAS, Bld. 38 Akademgorodok 50, Krasnoyarsk, 660036, Russia

ARTICLE INFO

Article history:
Received 17 January 2020
Received in revised form
11 May 2020
Accepted 25 May 2020
Available online 6 June 2020

Keywords:
Barbituric acids
Phenanthroline complexes
X-ray diffraction
Thermal
Spectroscopic and magnetic properties

ABSTRACT

Two new complexes $[Cu(Phen)_2(H_2O)](Hba)_2 \cdot 3H_2O$ (**1**) and $[Ni(Phen)_3](Htba)_2] \cdot Phen \cdot 2H_2O$ (**2**) (Phen = 1,10-phenanthroline, Hba^- = barbiturate ion, $Htba^-$ = thiobarbiturate ion) have been synthesized and characterized by elemental analysis, single-crystal and powder XRD, magnetic measurements, TG-DSC, FT-IR, and Vis absorption spectra. Complex **1** shows a distorted square pyramidal geometry around the copper (II) metal center. The coordination around the Ni atom is a distorted octahedron NiN_6. The 3D and 2D supramolecular structures of **1** and **2** are formed respectively by intermolecular H-bonds. Two N–H···O hydrogen bonds in **1**, and N–H···O, N–H···S hydrogen bonds in **2** form infinite chains. As a result of π–π interactions, similar 4-membered zigzag chains in structures **1** and **2** respectively are formed.

© 2020 Elsevier B.V. All rights reserved.

1. Introduction

Transition metal complexes containing phenanthroline (Phen) have been interesting for their applicability in catalysis [1], medicinal chemistry [2], photoelectronic and magnetic materials [3]. Attached to metal ions, the Phen ligands favor the intermolecular π–π stacking interactions with other aromatic molecules or ions, such as barbituric acids [4], which can play an important role in sustaining supramolecular solid-state architectures [5]. Barbituric (H_2ba) and 2-thiobarbituric (H_2tba) acids (Fig. 1S) are the parent molecules of 5,5-substituted barbiturates and thiobarbiturates, which are important groups of sedative/hypnotic drugs [6]. The Hba^- and $Htba^-$ anions possess good hydrogen-bonding acceptors and donors, and are prone to π–π interactions, which is important for molecular recognition and crystal design [7–10]. Design strategies simultaneously employing coordination bonds, hydrogen bonds, and π–π stacking interactions in crystal engineering are mostly not well documented so far [11]. The often so-called π–π interactions are in the order of 10 kcal mol^{-1}, thus further stabilizing the structural arrangement [12]. Within a systematic study of the metal barbiturate complexes, two mixed-ligand complexes, $[Cu(Phen)_2(H_2O)](Hba)_2 \cdot 3H_2O$ (**1**) and $[Ni(Phen)_3](Htba)_2 \cdot Phen \cdot 2H_2O$ (**2**), were prepared and studied. The main objective of this work is to compare the crystal structure of the synthesized complexes based on the analysis of supramolecular interactions (hydrogen bonds, π–π interactions) of uncoordinated Hba^- and $Htba^-$ ions with 1,10-phenanthroline.

2. Experimental section

2.1. Reagents and synthesis

1,10-phenanthroline monohydrate (CAS number: 5144-89-8),

* Corresponding author. Laboratory of Crystal Physics, Kirensky Institute of Physics, Federal Research Center KSC SB RAS, bld. 38 Akademgorodok 50, Krasnoyarsk, 660036, Russia.
E-mail address: msmolokeev@gmail.com (M.S. Molokeev).

https://doi.org/10.1016/j.molstruc.2020.128526
0022-2860/© 2020 Elsevier B.V. All rights reserved.

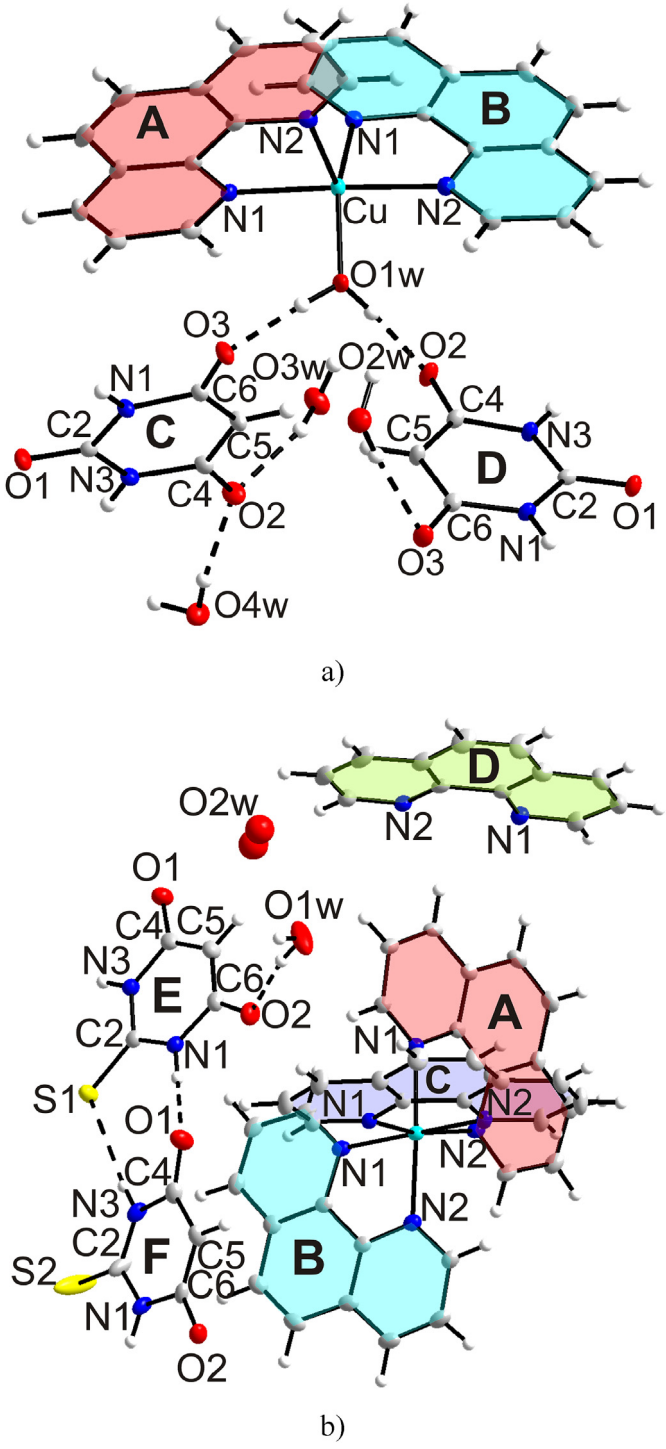

Fig. 1. The asymmetric unit of the $[Cu(Phen)_2(H_2O)](Hba)_2 \cdot 3H_2O$ (**1**) (a), $[Ni(Phen)_3](Htba)_2 \cdot Phen \cdot 2H_2O$ (**2**) (b) unit cell. Independent molecules are marked by labels (A–D). The intermolecular hydrogen bonds in **1** and **2** are represented by dashed lines. The ellipsoids are drawn at the 50% probability level, except for the hydrogen atoms represented by spheres.

barbituric acid (CAS number: 67-52-7) and 2-thiobarbituric acid (CAS number: 504-17-6) were commercially available from Sigma-Aldrich. $CuCl_2 \cdot 2H_2O$, $NiCO_3$, NaOH, acetone, ethyl alcohol and dimethyl sulfoxide were obtained as reagents of analytical grade (Acros) and they were also used without additional purification.

2.1.1. Synthesis of crystal 1

0.10 g (0.78 mmol) of barbituric acid in 5 ml of water was neutralized with an equimolar amount of solid NaOH (0.031 g, 0.78 mmol) at 90 °C for 5 min. To the resulting hot solution, 0.066 g of $CuCl_2 \cdot 2H_2O$ (0.39 mmol) and 0.155 g (0.78 mmol) of 1,10-phenanthroline monohydrate were added in turn with stirring. The produced bulk green precipitate dissolved after the copper salt was added to the reaction mixture, and the solution color changed from green to dark green. The resulting solution (~4 ml) was slowly cooled and allowed to evaporate at room temperature (pH 5). A day later, the dark green rectangular crystals were observed, which were filtered off and dried in air to a constant weight (yield: 63%). A single crystal for the X-ray diffraction analysis was taken directly from the total mass of the product. The elemental analysis for $C_{32}H_{30}CuN_8O_{10}$ (**1**): Calc.: C, 51.2%; H, 4.03%; N, 14.9%. Found: C, 50.8%; H, 4.21%; N, 14.6%. Complex **1** is soluble in water, alcohol, acetone and dimethyl sulfoxide.

2.1.2. Synthesis of crystal 2

To 2-thiobarbituric acid (0.1 g, 0.69 mmol) in 10 ml of water, a 5% excess of nickel carbonate (0.050 g, 3 mmol) was added, then the mixture was kept at 90 °C for 1 h and unreacted nickel carbonate was filtered off. To the hot green filtrate (6 ml), 1,10-phenanthroline monohydrate (0.206 g, 1.0 mmol) was added with stirring. The resulting mixture, consisting of a heavier red oil and an orange solution on top (pH 6), was slowly cooled and left at room temperature for 3 days. The formed stick-shaped red crystals of **2** were filtered and dried in the air to a constant weight (yield: 73%). A single crystal for X-ray diffraction analysis was taken directly from the crystalline precipitate. The elemental analysis for $C_{56}H_{40}N_{12}NiO_6S_2$ (**2**): Calc.: C, 61.2%; H, 3.67%; N, 15.3%, S, 5.83%. Found: C, 60.7%; H, 3.88%; N, 14.9%; S, 5.67%. Complex **2** is soluble in dimethyl sulfoxide, alcohol, acetone and water.

2.2. X-ray diffraction analysis

The intensity patterns were collected from single crystals **1** and **2** at 293 K using D8 Venture diffractometer (Bruker AXS) equipped with a CCD-detector, graphite monochromator and Mo Kα radiation source. The absorption corrections were applied using the SADABS program. The structures were solved by the direct methods using the SHELXS package and refined in the anisotropic approach for non-hydrogen atoms using the SHELXL program [13]. All hydrogen atoms in **1** and almost all in **2** were found with the Fourier difference maps. Hydrogen atoms of one disordered water molecule were not localized in structure **2**. Further, the hydrogen atoms which are linked with C,N atoms in the **1** and **2** were positioned geometrically as riding on their parent atoms with d (C–H) = 0.93–0.98 Å, d (N–H) = 0.89 Å depending on geometry and $U_{iso}(H) = 1.2U_{eq}$ (C,N). The structure test for the presence of missing symmetry elements and possible voids was carried out with the PLATON program [14]. For the crystal structure plotting, the DIAMOND software [15] was used.

The powder X-ray diffraction data of **1** and **2** were obtained using the D8 ADVANCE diffractometer ((Bruker, analytical equipment of the Center for Collective Use of KSC SB RAS) equipped with a VANTEC detector with a Ni filter. The measurements were made using Cu Kα radiation. The structural parameters defined by single crystal analysis were used as a baseline in powder pattern Rietveld refinement. The refinement was carried out with the TOPAS program [16]. Low R-factors and good refinement results shown in (Fig. 2S) indicate the crystal structures of the powder samples to be representative one of the **1** and **2** bulk structure.

2.3. Physical measurements

TGA was carried out on the simultaneous SDT-Q600 thermal analyzer (TA Instruments, USA) under the dynamic air atmosphere (50 ml/min flow rate) within 25–800 °C at the scan rate of 10 °C/min. The qualitative composition of the evolved gases was determined by the Nicolet380 FT-IR spectrometer (Thermo Scientific, USA) combined with a thermal analyzer and the TGA/FT-IR interface (gas phase analysis attachment). This set up allows simultaneous accumulation of the DTA/TG data and the released gas

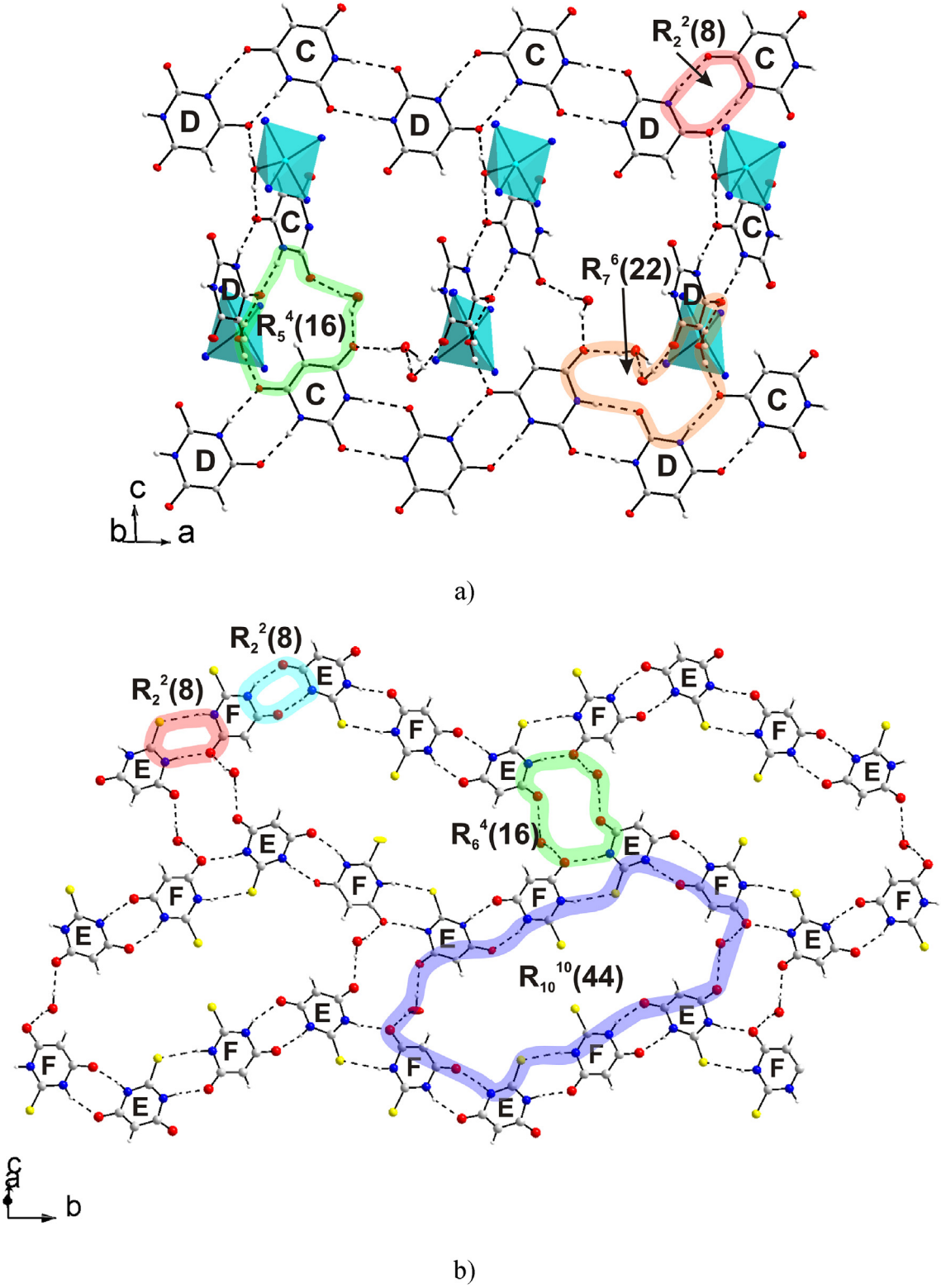

Fig. 2. Hydrogen bonding in **1** (a) and **2** (b). The H-bonds are marked by dashed lines, the H-bond motifs are marked by circles.

composition. The compound weight was 7.044 mg for **1** and 6.930 mg for **2**. Platinum crucibles with perforated lids were used as containers. The IR spectra were recorded as KBr pellets on the Nicolet 6700 FT-IR spectrometer (Thermo Scientific, USA, SFU CEJU, School of Petroleum and Gas Engineering) in the of 400–4000 cm^{-1} region. UV–Vis spectra were recorded on the Evolution 300 spectrophotometer (Thermo Scientific, UK). Magnetic measurements were performed on the MPMS-XL SQUID magnetometer in magnetic fields up to 50 kOe at temperatures of 5, 15 and 50 K. The chemical analysis was carried out with the HCNS-0 EA 1112 Flash Elemental Analyser.

3. Results and discussion

3.1. Crystal structure of 1

Complex $[Cu(Phen)_2(H_2O)](Hba)_2 \cdot 3H_2O$ (**1**) crystallizes in a monoclinic system and its structure is solved in the space group *Cc*. The crystal structure of **1** consists of a mononuclear $[Cu(Phen)_2(H_2O)]^{2+}$ cation and two barbiturate counter anions and three crystallization water molecules. The main crystal data are shown in Table 1. The main detected bond lengths are shown in Table 1S.

The asymmetric unit cell contains one Cu^{2+} ion, two Phen molecules, two Hba^- ions and four H_2O molecules (Fig. 1a). The Cu^{2+} ion is coordinated by one H_2O molecule and two Phen molecules through four N atoms. The bond lengths are *d* (Cu–N) = 1.996(3)–2.183(2) Å and *d* (Cu–Ow) = 1.958(2) Å, which are close to the corresponding distances in other compounds containing the $[Cu(Phen)_2(H_2O)]^+$ cation [3,5,17–20]. The N1A–Cu–N2A and N1B–Cu–N2B bond angles are 79.66(8)° and 81.92(9)°. In this structure, N4O surrounding the metal may be described as intermediate between distorted square pyramidal with the most distant from the metal nitrogen atom N2A in the apical position and distorted trigonal bipyramidal, where two proximate nitrogen atoms N1A and N2B. The distortion degree is indicated by the general descriptor $\tau = (\beta - \alpha)/60$ for the five-coordinated complexes, where α and β are the two largest angles at the metal center. If τ ranges from 0 to 0.5, the molecular geometry is distorted square pyramidal, while the value of τ between 0.5 and 1 indicates that the molecular geometry is distorted trigonal bipyramidal [21–23]. In complex **1**, τ is 0.41; therefore, the five-coordinated Cu(II) ion shows a distortion of the square pyramidal geometry. The axial position is occupied by the N2A atom of coordinated Phen molecule, *d* (Cu–N2A) = 2.183(2) Å. The axial Cu–N distance is quite longer than the equatorial ones (1.996(3), 2.015(2) and 2.017(2) Å). The elongation of the apical bond length in complex **1** is of comparable magnitude to that observed in the previously reported square pyramidal complexes [5,18]. The N2B–Cu–N1A angle is 176.64(10)°. The angles around the copper (II) atom in the basal plane vary from 101.71(7)° to 152.17(8)°, which indicates a strongly distorted geometry. The dihedral angle between the chelate Phen ligands is 69.46(7)°. The barbiturate anions are located in the outer-sphere. The main C–O, C–N, C–C bond lengths (Table 1S) and the angles in them coincide with those found earlier in other related compounds containing uncoordinated Hba^- ions [24–27]. Crystallization water fills the voids between the $[Cu(Phen)_2(H_2O)]^{2+}$ cations.

There are four N–H···O and eight O–H···O hydrogen bonds in the structure **1** (Table 2S) which form a 3D network. All hydrogen atoms of all water molecules are involved in hydrogen bonding. This is a 4-nodal net with stoichiometry (3-c) (4-c) (5-c) (6-c) and with vertex symbol (3.4^2) ($3.4^3.5.6.7^3.8^2.9^2.10^2$) ($3^2.4.5^2.6$) ($3^2.4^2.5^2.6.7^3$) which is unknown in the ToposPro database [28]. The 2D layer in the plane based on *a*–*b* and *c* axis with supramolecular motifs $R_2^2(8)$, $R_5^4(16)$ and $R_7^6(22)$ can be marked (Fig. 2a). N–H···O

Table 1
Crystal structure parameters of **1** and **2**.

Single crystal	$[Cu(Phen)_2(H_2O)](Hba)_2 \cdot 3H_2O$	$[Ni(Phen)_3](Htba)_2 \cdot Phen \cdot 2H_2O$
Moiety formula	$C_{32}H_{30}CuN_8O_{10}$	$C_{56}H_{40}N_{12}NiO_6S_2$
Dimension (mm)	0.48 × 0.25 × 0.12	0.50 × 0.40 × 0.15
Color	green	red
Molecular weight	750.18	1099.83
Temperature (K)	293	293
Space group, *Z*	*Cc*, 4	$P2_1/n$, 4
a (Å)	17.1196 (4)	13.5359 (5)
b (Å)	12.2262 (3)	21.3738 (8)
c (Å)	14.9531 (4)	17.8164 (6)
α (°)	90	90
β (°)	92.989 (1)	103.023 (1)
γ (°)	90	90
V (Å^3)	3125.54 (13)	5022.0 (3)
ρ_{calc} (g/cm^3)	1.594	1.455
μ (mm^{-1})	0.774	0.536
Reflections measured	35454	189270
Reflections independent	8882	14721
Reflections with $F > 4\sigma(F)$	8533	11287
$2\theta_{max}$ (°)	60.14	60.14
h, *k*, *l* - limits	$-24 \le h \le 24$; $-17 \le k \le 17$; $-21 \le l \le 20$	$-18 \le h \le 19$; $-30 \le k \le 30$; $-25 \le l \le 24$
R_{int}	0.0306	0.0633
The weighed refinement of F^2	$w = 1/[\sigma^2(F_o^2)+(0.0434P)^2+0.8913P]$, $P = (F_o^2+2F_c^2)/3$	$w = 1/[\sigma^2(F_o^2)+(0.0721P)^2+8.74P]$, $P = (F_o^2+2F_c^2)/3$
Number of refinement parameters	485	700
$R1$ [$F_o > 4\sigma(F_o)$]	0.0266	0.0555
w*R*2	0.0679	0.1376
Goof	1.024	1.015
$\Delta\rho_{max}$ (e/Å^3)	0.321	3.028
$\Delta\rho_{min}$ (e/Å^3)	−0.666	−2.245
$(\Delta/\sigma)_{max}$	0.000	0.000

Table 2
The magnetizations and the number of magnetic particles.

Magnetic ion	M (erg/Oe)	N (un./g)	N (un./cm^3)
Cu^{2+}	$2.104\bullet10^{-20}$	$6.164\bullet10^{20}$	$3.867\bullet10^{20}$
Ni^{2+}	$3.150\bullet10^{-20}$	$4.09\bullet10^{20}$	$2.81\bullet10^{20}$

hydrogen bonds form the infinite chains of Hba^-along axis *a* based on the $R_2^2(8)$ pattern. These chains are linked by Ow–H···O hydrogen bonds. Coordinated Phen molecules are not involved in H-bonding. In addition, there are the π–π interactions between the rings of Phen molecules and Hba^- ions (Fig. 3a, Table 3S) that form discrete units. The interplanar separation of Phen ligands (A, B) in the centrosymmetric pattern with overlapping phenyl–phenyl rings is 3.3833(10) Å, and centroid···centroid distance is 3.5309(14) Å thus indicating the slipping stacking interaction with offset. Moreover, each phenanthroline molecule is bound by $phenyl_{(Phen)}$–Hba^- π–π interaction with one barbiturate ion forming a zigzag Hba^-–Phen–Phen–Hba^- chain. The interplanar separations of Phen and Hba^- in the pattern with overlapping phenyl rings are 3.2886(10), 3.4905(13) Å, and centroid···centroid distances are 3.4905(13), 3.6019(13) Å. It should be noted that the same 4-membered Hba^-–Phen–Phen–Hba^- chains are also formed in the structure $[Co(Phen)_2(H_2O)_2](Hba)_2\cdot2H_2O$ [27]. Similar chains of Hba^-–Bipy–Bipy–Hba^- (Bipy = 2,2′-bipyridine) are also found in the complexes $[Cu_2(Bipy)_2(H_2O)_2(OH)_2](Hba)_2\cdot2H_2O$ and [Cu(Bipy)(H_2O) (Hba)Cl]$\cdot2H_2O$ [29].

3.2. Crystal structure of 2

Complex $[Ni(Phen)_3]Phen(Htba)_2\cdot2H_2O$ (**2**) crystallizes in a monoclinic system and the structure is solved in the space group $P2_1/n$. The crystal structure of **2** consists of a mononuclear $[Ni(Phen)_3]^{2+}$ cation, two thiobarbiturate counter anions, uncoordinated Phen and two water molecules. Details of the data collection and the parameters of the refinement process are presented in Table 1. Selected bond lengths are listed in Table 1S.

The asymmetric unit contains one Ni^{2+} ion, four Phen molecules, two $Htba^-$ ions and two H_2O molecules (Fig. 1b). One of the two water molecules is disordered over two positions. The Ni^{2+} ion is coordinated by three Phen molecules through six N atoms, forming NiN_6 octahedron with *d* (Ni–N) = 2.076(2)–2.124(2) Å which is also falls into the interval obtained for other pre-characterized compounds containing $[Ni(Phen)_3]^{2+}$ cation [30]. These values are slightly bigger than *d* (Ni–N) 2.054(2)–2.055(2) Å, acquired earlier for [Ni(Phen)$(H_2O)_3$Br]Br compound [27]. A possible reason for the greater distance *d* (Ni–N) in **2** is the greater mutual repulsion between the three coordinated Phen ligands. The dihedral angle between the chelate ligands A and B, A and C, B and C are 66.40(8), 72.53(5), 80.70(8)° respectively. Water molecules are mainly located between the layer shown in Fig. 2b and the layer of $[Ni(Phen)_3]^{2+}$ cations. Complex **2**, as well as **1** has a discrete structure. One of the four 1,10-phenanthroline molecules in **2** does not form a chemical bond with nickel ions. $Htba^-$ anions compensating the $[Ni(Phen)_3]^{2+}$ cation charge, like one of the 1,10-phenanthroline molecule, are located in the outer sphere. As in **1**, the main C–O, C–N, C–C bond lengths (Table 1S) and the angles in barbiturate ions coincide with those found in other complexes containing uncoordinated $Htba^-$ ions [26,31,32].

There are three N–H···O, one N–H···S and two O–H···O hydrogen bonds in the structure (Fig. 2b, Table 2S) forming a 2D network. $Htba^-$ anions form infinite chains of Hba^- along axis *b*

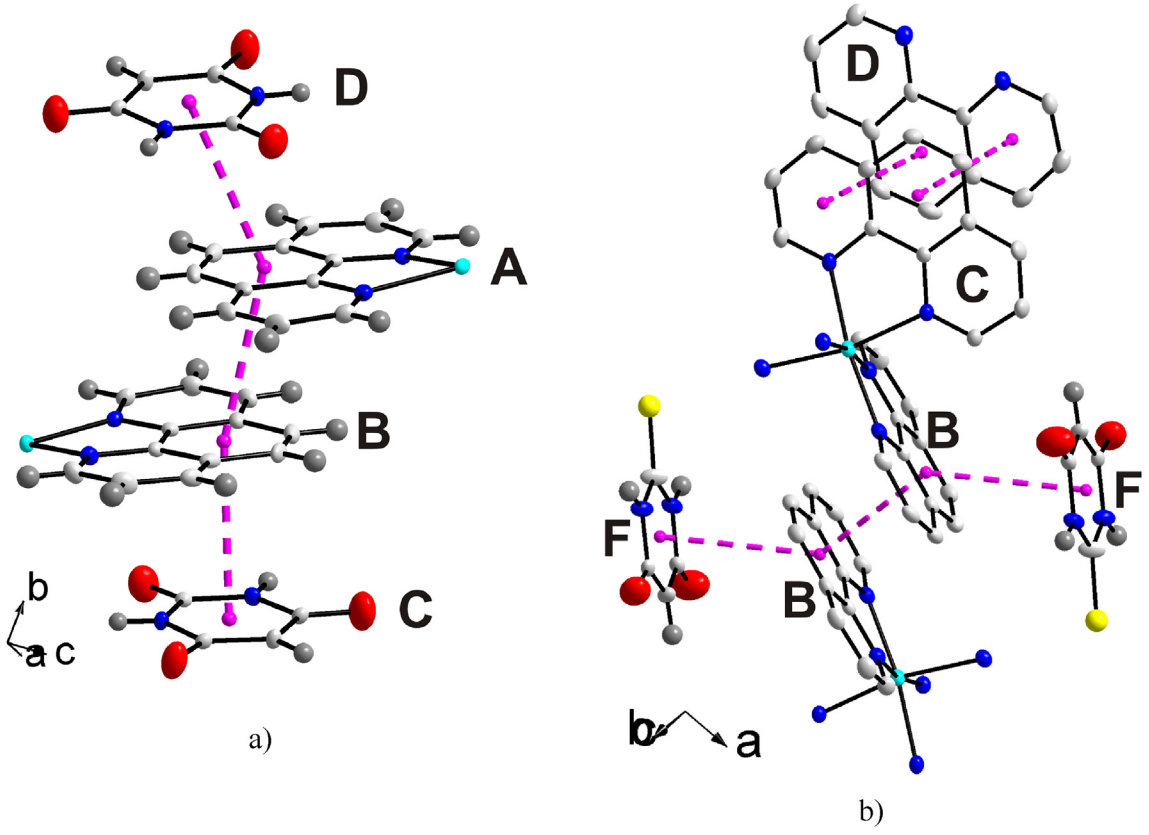

Fig. 3. π–π interactions in **1** (a) and **2** (b). Some hydrogen atoms in figure (b) were omitted for the picture clarity.

based on the R_2^2 (8) pattern. These chains are interconnected by pairs Ow–H···O hydrogen bonds. Since the hydrogen atoms of disordered H_2O molecule were not localized, some hydrogen bonds were missed. Anyway, the present hydrogen 2D net was analyzed. This net is an uninodal 3-c net with vertex symbol (4.8^2) known as *fes* net in the ToposPro database [28]. Moreover, there are π–π interactions between the rings of Phen molecules and Hba^- ions. There are π–π interactions between the rings of B phenanthroline molecules coordinated to different nickel ions and Hba^- ions in **2** (Fig. 3b, Table 3S) forming 4-member chains $Htba^-$–Phen–Phen–$Htba^-$. A similar interaction pattern is also established in complex **1**. As $[Cu(Phen)_2(H_2O)]^{2+}$ cations in **1**, the $[Ni(Phen)_3]^{2+}$ cations are united into pairs by π–π interaction between the neighboring Phen of a head-to-tail type (Fig. 3b). The interplanar separation of Phen ligands B in the centrosymmetric pattern with overlapping of phenyl–phenyl rings is 3.4188(9) Å, and centroid···centroid distance is 3.6155(13) Å thus indicating the slipping stacking interaction with offset. In addition, each phenanthroline molecule is bound by $phenyl_{(Phen)}$–$Htba^-$ π–π interaction with one barbiturate ion. The interplanar separation of Phen (B) and $Htba^-$ (F) in the pattern with overlapping of phenyl rings is 3.8892(9) Å, and centroid···centroid distance is 3.9724(14) Å. Uncoordinated D phenanthroline molecule is also involved in π–π interactions with the coordinated C phenanthroline molecule. The interaction involves one phenyl and one pyridine ring of each Phen molecule. The interplanar separations of these Phen molecules in the pattern with overlapping of phenyl–pyridine rings are 3.5469(10) and 3.7595(10) Å, and centroid···centroid distances are 3.7637(14), 3.9327(15) Å. In addition to complex **2**, only two structurally characterized complexes contain simultaneously coordinated and uncoordinated phenanthroline molecules [30]. In $\{Ni(Phen)_3\}_2[V_{14}Sb_8O_{42}]\cdot Phen\cdot 12H_2O$ [33] π–π interactions between the $[Ni(Phen)_3]^{2+}$ cations form an infinite chain (Fig. 3S). The cationic layer in $\{Ni(Phen)_3\}_2[V_4O_{12}]\cdot Phen\cdot 22H_2O$ [34] is also stabilized by π–π interactions between phenanthroline molecules, both coordinated to the central atom and uncoordinated solvate molecules.

3.3. Spectroscopic study

The IR spectra of the complexes (Figs. 4S–5S) were analyzed using data from Ref. [25,26,35–37]. They are significantly different from the spectra of starting reagents, thereby indicating the formation of new compounds. In the IR spectrum of **1** (Fig. 4S, curve 3), the broad bands centered at 3530 and 3383 cm^{-1} are assigned to the ν(OH) stretching vibrations of coordinated and crystallization water molecules [35], which fits the results of elemental and thermal analyses. A broad band centered at 3086 cm^{-1} is assigned to the ν(NH) stretching vibrations of Hba^- ions. The vibration bands centered at 1519, 1429 and 1355 cm^{-1} in IR spectra of **1** and 1515, 1449 and 1353 cm^{-1} in IR spectra of **2** indicate the presence of 1,10-phenanthroline. In the IR spectrum of complex **2** (Fig. 5S, curve 3), the bands at 3386 and 3550 cm^{-1} are assigned to the ν(OH) vibrations of water molecules and a broad band centered at 3167 cm^{-1} is assigned to the ν(NH) stretching vibrations of $Htba^-$ ions. The bands with the frequencies 1682 and 1609 cm^{-1} in the IR spectra **1** and **2** respectively are assigned to the stretching mode of CO in Hba^- and $Htba^-$ ions [25,26]. Peaks at 431 and 426 cm^{-1} in the spectra of **1** and **2** respectively are attributed to the M – N stretching vibrations [37]. IR spectra of the complexes **1** and **2** are well-aligned with the result obtained by single crystal X-ray diffraction. The electronic spectra of **1** (Figs. 6S) and **2** (Fig. 7S), in DMSO, show broad bands in the 650–800 nm and 440–490 nm range of MLCT character, centered at 740 and 452 nm, respectively. The d–d* spectra of aqueous solutions exhibit a broad band in the range 550–800 nm centered at ca. 730 nm for **1** and a broad band in the range 460–580 nm centered at ca. 520 nm for **2**, which are consistent with the presence of the Cu(II) chromophore with distorted square-pyramidal geometry and Ni(II) chromophore with octahedral geometry [38]. The broad band at λ_{max} = 740 nm in DMSO and 730 nm in water is assigned to $^2E_g \rightarrow {}^2T_{2g}$ transition of Cu(II) (d^9). The response band at λ_{max} = 452 nm in DMSO and 520 nm in water is assigned to d–d* transition of Ni(II) ion (d^8) [$^3A_{2g} \rightarrow {}^3T_{1g}$(P)] [38,39].

3.4. Magnetic properties

The results of magnetization (M) measurements of the copper-containing (part 1) and nickel-containing (part 2) polycrystals (experimental points) are shown in Fig. 8S. The temperature dependences of the magnetization for both magnetic ions (part a) are qualitatively similar, and give reason to consider them as paramagnets. The field dependences of the magnetization for complexes **1** and **2** (part b) also have a similar nature. The experimental magnetization dependences were fitted by the Langevin function [40].

$$M = Nm[\coth(mH/K_BT) - (K_BT/mH)],$$

where N is the number of magnetic particles per mass and volume unit, m is the magnetic moment of the particle, K_B is the Boltzmann constant, T and H are temperature and magnetic field strength, respectively. Table 2 shows the values of the magnetic moment and the number of magnetic particles in **1**–**2**.

3.5. Thermal decomposition

Thermal decomposition of complexes **1** and **2** started with the release of water molecules, which was confirmed by the IR spectroscopic analysis of released gases. In **1**, an experimental weight loss (Δm) of 10.0% is observed between 75 and 175 °C (Fig. 9S), which corresponds to the release of the coordinated and crystallization water molecules ($-4H_2O$, Δm_{theor} = 9.61%). At T > 250 °C, the oxidative decomposition of $[Cu(Phen)_2(H_2O)](Hba)_2\cdot 3H_2O$ (**1**) most likely begins, accompanied by the strong exothermic effect at 509.7 °C. At 650 °C, the final product consists mainly of copper (II) oxide CuO (Fig. 10S). The total Δm was found to be 90.1%, which is bigger than that calculated for the transformation of **1** to CuO (Δm_{theor} = 89.4%), the difference may be due to the impurities in the analyzed sample and the thermolysis product. The DSC and TG curves of $[Ni(Phen)_3](Htba)_2\cdot Phen\cdot 2H_2O$ (**2**) show two-step dehydration (Fig. 11S) which is accompanied by an endo effect at 141.3 °C. The first dehydration stage proceeded in the range of 75–130 °C, which corresponds to the release of the lattice water molecule with Δm = 1.4% ($-H_2O$, Δm_{theor} = 1.6%). The second dehydration stage in the range of 130–150 °C showed Δm = 1.5% ($-H_2O$, Δm_{theor} = 1.6%). At T > 210 °C, the oxidative decomposition of **2** is accompanied by four exothermic effects, the strongest of which registered at 607.8 °C. At 680 °C, the final product consists mainly of nickel oxide NiO (Fig. 12S). The total experimental weight loss was found to be 94.0%, which is bigger than that calculated for the transformation of **2** to NiO (Δm_{theor} = 93.2%). As in **1**, the difference may be due to the impurities in the analyzed sample and thermolysis product.

4. Conclusions

Two mixed-ligand Cu(II) and Ni(II) complexes with compositions $[Cu(Phen)_2(H_2O)](Hba)_2\cdot 3H_2O$ (**1**) and $[Ni(Phen)_3](Htba)_2\cdot Phen\cdot 2H_2O$ (**2**) were prepared and studied. In **1**, the five-

coordinated Cu(II) ion shows a distortion of square pyramidal geometry. The coordination around the Ni atom is a distorted octahedron, expected because of the presence of the rigid Phen ligand. Non coordinating counterions Hba^- and $Htba^-$ are in the outer sphere of these complexes. The intermolecular hydrogen bonds N–H···O, O–H···O in the structure **1** and N–H···O, O–H···O, N–H···S in the structure **2** form a 3D and 2D network, respectively. In structures, the Hba^- and $Htba^-$ ions are connected by hydrogen bonds in the infinite zigzag chains based on the $R_2^2(8)$ pattern. In **1**–**2**, the centrosymmetric $R_2^2(8)$ pattern is formed by two N–H···O hydrogen bonds. In addition, in **2**, it is formed using one N–H···O and N–H···S hydrogen bonds, with the different atomic composition patterns following each other in a chain (Fig. 2a). In **1**, the chains of Hba^- ions are linked via N–H … $O_{Hba(chain\ 1)}$ … H–Ow–H … $O_{Hba(chain\ 2)}$ interactions. In **2**, the chains of $Htba^-$ are connected by one water molecule, which is a donor of two hydrogen bonds. Phen molecules in the complexes do not participate in hydrogen bonds. The π–π interactions also contribute to the stabilization of structures. The cations $[Cu(Phen)_2(H_2O)]^{2+}$ in **1** and $[Ni(Phen)_3]^{2+}$ in **2** are connected in pairs by π–π interaction between two neighboring Phen molecules, each of which, in turn, is involved in the π–π interaction with anion Hba^- and $Htba^-$, respectively, with the formation of 4-membered chains X–Phen–Phen–X (X = Hba^- and $Htba^-$). In **2**, the uncoordinated phenanthroline molecule and $[Ni(Phen)_3]^{2+}$ cation are bound by π–π interaction. The spectroscopic, magnetic and thermal properties of **1**–**2** are consistent with the X-ray results.

CRediT authorship contribution statement

Nicolay N. Golovnev: Conceptualization, Methodology, Writing - original draft, Writing - review & editing, Visualization. **Maxim S. Molokeev:** Conceptualization, Methodology, Writing - original draft, Writing - review & editing, Visualization, Funding acquisition. **Irina V. Sterkhova:** Investigation, Visualization. **Maxim K. Lesnikov:** Investigation, Visualization. **Anastasia V. Demina:** Investigation, Visualization. **Gennady S. Patrin:** Investigation, Visualization, Writing - review & editing.

Acknowledgements

The study was funded by RFBR according to the research project № 19-52-80003. X-ray data from single crystals were obtained with use the analytical equipment of Baikal Center of collective use of SB RAS and powder pattern were obtained with use the analytical equipment of Krasnoyarsk Center of collective use of SB RAS.

Supplementary data

The crystallographic data (excluding structure factors) for the structural analysis have been deposited with Cambridge Crystallographic Data Center (**1** - CCDC # 1962890; **2** - CCDC # 1962891). The information may be obtained free of charge from The Director, CCDC, 12 Union Road, Cambridge CB2 1EZ, UK (Fax: +44 (1223) 336–033, E-mail: deposit@ccdc.cam.ac.uk, or www.ccdc.cam.ac.uk).

Appendix A. Supplementary data

Supplementary data to this article can be found online at https://doi.org/10.1016/j.molstruc.2020.128526.

References

[1] B. Louis, C. Detoni, N.M.F. Carvalho, C.D. Duarte, O.A.C. Antunes, Cu(II) bipyridine and phenantroline complexes: tailor-made catalysts for the selective oxidation of tetralin, Appl. Catal. 360 (2009) 218–225, https://doi.org/10.1016/j.apcata.2009.03.022.
[2] R.N. Patel, Y.P. Singh, Y. Singh, R.J. Butcher, Synthesis, crystal structure, DFT computation and bioactivity measurements of copper (II) polypyridyl complexes, Polyhedron 104 (2016) 116–126, https://doi.org/10.1016/j.poly.2015.11.042.
[3] L.N. Ashbrook, C.M. Elliott, Dye-sensitized solar cell studies of a donor-appended bis (2,9-dimethyl-1,10-phenanthroline) Cu(I) dye paired with a cobalt-based mediator, J. Phys. Chem. C 117 (2013) 3853–3864, https://doi.org/10.1021/jp3123693.
[4] N.N. Golovnev, M.S. Molokeev, I.V. Sterkhova, M.K. Lesnikov, Novel 1,3-diethyl-2-thiobarbiturates of 2,2′-bipyridine and 1,10-phenanthroline: synthesis, crystal structure and thermal stability, J. Mol. Struct. 1171 (2018) 488–494, https://doi.org/10.1016/j.molstruc.2018.06.035.
[5] A. Crispini, C. Cretu, D. Aparaschivei, A.A. Andelescu, V. Sasca, V. Badea, I. Aiello, E.I. Szerb, O. Costisor, Influence of the counterion on the geometry of Cu(I) and Cu(II) complexes with 1,10-phenanthroline, Inorg. Chim. Acta. 470 (2018) 342–351, https://doi.org/10.1016/j.ica.2017.05.064.
[6] E.N. Padeiskaya, Prevention, Diagnosis, and Pharmacotherapy of Some Infectious Diseases, Bioinform, Moscow, 2002 (in Russian).
[7] K.T. Mahmudov, M.N. Kopylovich, A.M. Maharramov, M.M. Kurbanova, A.V. Gurbanov, A.J.L. Pombeiro, Barbituric acids as a useful tool for the construction of coordination and supramolecular compounds, Coord. Chem. Rev. 265 (2014) 1–37, https://doi.org/10.1016/j.ccr.2014.01.002.
[8] N.N. Golovnev, M.S. Molokeev, 2-Thiobarbituric Acid and its Complexes with Metals: Synthesis, Structure and Properties, Siberian Federal University, Krasnoyarsk, 2014, ISBN 978-5-7638-3080-4 (in Russian).
[9] M. Mitra, P. Manna, A. Bauzá, P. Ballester, S.K. Seth, S.R. Choudhury, A. Frontera, S. Mukhopadhyay, 3-Picoline mediated self-assembly of M(II)–Malonate complexes (M= Ni/Co/Mn/Mg/Zn/Cu) assisted by various weak forces involving lone pair–π, π–π, and anion··· π–hole interactions, J. Phys. Chem. 118B (2014) 14713–14726, https://doi.org/10.1021/jp510075m.
[10] X.Y. Yu, X. Zhang, Z.G. Liu, X.B. Cui, J.N. Xu, Y.H. Luo, Syntheses and structures of three supramolecular complexes based on 2-(pyridine-2-yl)-1H-imidazole-4, 5-dicarboxylic acid, J. Mol. Struct. 1147 (2017) 747–753, https://doi.org/10.1016/j.molstruc.2017.07.012.
[11] H.W. Roesky, M. Andruh, The interplay of coordinative, hydrogen bonding and π–π stacking interactions in sustaining, Coord. Chem. Rev. 236 (2003) 91–119, https://doi.org/10.1016/S0010-8545(02)00218-7.
[12] J. Hilbert, C. Näther, W. Bensch, Utilization of mixtures of aromatic N-donor ligands of different coordination ability for the solvothermal synthesis of thiostannate containing molecules, Dalton Trans. 44 (2015) 11542–11550, https://doi.org/10.1039/C5DT01145K.
[13] G.M. Sheldrick, A short history of SHELX, Acta Crystallogr. A64 (2008) 112–122, https://doi.org/10.1107/S0108767307043930.
[14] A.L. Spek, Single-crystal structure validation with the program PLATON, Appl.Cryst. 36 (2003) 7–13.
[15] K. Brandenburg, M. Berndt, DIAMOND – Visual Crystal Structure Information System CRYSTAL IMPACT, Postfach 1251, D-53002 Bonn.
[16] Bruker AXS Topas, V4: General Profile and Structure Analysis Software for Powder Diffraction Data. – User's Manual, Bruker AXS, Karlsruhe, Germany, 2008.
[17] D.V. Scaltrito, D.W. Thompson, J.A. O'Callaghan, G.J. Meyer, MLCT excited states of cuprous bis-phenanthroline coordination compounds, Coord. Chem. Rev. 208 (2000) 243–266, https://doi.org/10.1016/S0010-8545(00)00309-X.
[18] A.M. Madalan, V.Ch Kravtsov, D. Pajic, K. Zadro, YuA. Simonov, N. Stanica, L. Ouahab, J. Lipkowski, M. Andruh, Complexes containing $[Cu(AA)(BB)]^+$ moieties (AA = acetylacetonate, salicylaldehydate; BB = 1,10-phenanthroline, Me_2bipy = 4,4′-Dimethyl-2,2′-bipyridine), Inorg. Chim. Acta. 357 (2004) 4151–4164, https://doi.org/10.1016/j.ica.2004.06.010.
[19] Y. Liu, Y. Bi, W. He, X. Wang, W. Liao, H. Zhang, A copper/p-sulfonatocalix arene/phenanthroline supramolecular compound with 1D $[Cu_2$-calixarene$]_n$ coordination chains, J. Mol. Struct. 919 (2009) 235–238, https://doi.org/10.1016/j.molstruc.2008.09.006.
[20] E. Melnic, E.B. Coropceanu, O.V. Kulikova, A.V. Siminel, D. Anderson, H.J. Rivera-Jacquez, A.E. Masunov, M.S. Fonari, V.Ch Kravtsov, Robust packing patterns and luminescence quenching in mononuclear $[Cu(II)(phen)_2]$ sulfates, J. Phys. Chem. C118 (2014) 30087–30100, https://doi.org/10.1021/jp5085845.
[21] L. Sacconi, Five coordination in 3d metal complexes, Pure Appl. Chem. 17 (1968) 95–128.
[22] S. Tanase, I.A. Koval, E. Bouwman, R.G.J. Reedijk, Ligand conformation enforces trigonal bipyramidal coordination geometry in a new dinuclear bis(pyrazolato)-bridged copper(II) complex: synthesis, crystal structure, and properties of $[Cu(Npy_2pz)]_2(ClO_4)_2\cdot 2CH_3CN$, Inorg. Chem. 44 (2005) 7860–7865, https://doi.org/10.1021/ic050793w.
[23] A.W. Addison, T.N. Rao, J.R. Reedijk, J. Rijn, G.C. Verschoor, Synthesis, structure, and spectroscopic properties of Copper(II) compounds containing nitrogen sulfur donor ligands–the crystal and molecular-structure of aqua 1,7-bis (N-methylbenzimidazol-2'-yl)-2, 6-dithiaheptane Copper(II) perchlorate, J. Chem. Soc. Dalton Trans. (1984) 1349–1356, https://doi.org/10.1039/DT9840001349. http://pubs.rsc.org.
[24] H.C. Garcia, R. Diniz, M.I. Yoshida, L.F.C. de Oliveira, Synthesis, structural studies and vibrational spectroscopy of Fe^{2+} and Zn^{2+} complexes containing

4,4′-bipyridine and barbiturate anion, J. Mol. Struct. 978 (2010) 79–85, https://doi.org/10.1016/j.molstruc.2010.01.035.
[25] H.C. Garcia, F.B. de Almeida, R. Diniz, M.I. Yoshida, L.F.C. de Oliveira, Supramolecular structures of metal complexes containing barbiturate and 1,2-bis(4-pyridyl)-ethane, J. Coord. Chem. 64 (2011) 1125–1138, https://doi.org/10.1080/00958972.2011.562894.
[26] N.N. Golovnev, M.S. Molokeev, M.K. Lesnikov, I.V. Sterkhova, V.V. Atuchin, Thiobarbiturate and barbiturate salts of pefloxacin drug: growth, structure, thermal stability and IR-spectra, J. Mol. Struct. 1149 (2017) 367–372, https://doi.org/10.1016/j.molstruc.2017.08.011.
[27] N.N. Golovnev, M.S. Molokeev, I.V. Sterkhova, M.K. Lesnikov, Two novel mixed-ligand Ni(II) and Co(II) complexes with 1,10-phenanthroline: synthesis, structural characterization, and thermal stability, Chem. Phys. Lett. 708 (2018) 11–16, https://doi.org/10.1016/j.cplett.2018.07.058.
[28] V.A. Blatov, A.P. Shevchenko, D.M. Proserpio, Applied topological analysis of crystal structures with the program package ToposPro, Cryst. Growth Des. 14 (2014) 3576–3586, https://doi.org/10.1021/cg500498k.
[29] N.N. Golovnev, M.S. Molokeev, I.V. Sterkhova, M.K. Lesnikov, Crystal structures of $[Cu_2$ (2,2′-bipyridine-N,N′)$_2(H_2O)_2(\mu_2$-OH)$_2$](barbiturate)$_2\cdot 2H_2O$ and [Cu(2,2′-bipyridine-N, N′)(H_2O)(barbiturate-O)Cl]$\cdot 2H_2O$, Inorg. Chem. Commun. 97 (2018) 88–92, https://doi.org/10.1016/j.inoche.2018.09.011.
[30] Cambridge Structural Database, Univ. of Cambridge, Cambridge, UK, 2019.
[31] N.N. Golovnev, M.S. Molokeev, M.K. Lesnikov, Crystal structure and properties of levofloxacinium 2-thiobarbiturate trihydrate, J. Struct. Chem. 59 (2018) 646–651, https://doi.org/10.1134/S0022476618030204.
[32] N.N. Golovnev, M.S. Molokeev, M.K. Lesnikov, V.V. Atuchin, Two salts and the salt cocrystal of ciprofloxacin with thiobarbituric and barbituric acids: the structure and properties, J. Phys. Org. Chem. 31 (2018) 1–11, https://doi.org/10.1002/poc.3773.
[33] M. Wendt, C. Näther, W. Bensch, High nuclearity antimonato-polyoxovanadate cluster $\{V_{15}Sb_6O_{42}\}$ as a synthon for the solvothermal in situ generation of α-and β-$\{V_{14}Sb_8O_{42}\}$ isomers, Chem. Eur J. 22 (2016) 7747–7751, https://doi.org/10.1002/chem.201601401.
[34] L. Zurkova, R. Kucsera, R. Gyepes, M. Sivak, Synthesis and X-ray crystal structure of two novel complexes: [MII(phen)$_3$]$\cdot 2V_4O_{12}\cdot$phen$\cdot 22H_2O$ (MII = Co, Ni; phen = phenanthroline), Monatsh. Chem. 134 (2003) 1071–1079, https://doi.org/10.1007/s00706-003-0030-4.
[35] K. Nakamoto, Infrared and Raman Spectra of Inorganic and Coordination Compounds, sixth ed., Wiley, New York, 2009, p. 419.
[36] T.P. Gerasimova, S.A. Katsyuba, Bipyridine and phenanthroline IR-spectral bands as indicators of metal spin state in hexacoordinated complexes of Fe(II), Ni(II) and Co(II), Dalton Trans. 42 (2013) 1787–1797, https://doi.org/10.1039/C2DT31922E.
[37] S.-R. Fan, L.-G. Zhu, Secondary synthesis of two cobalt complexes by the use of 5-sulfosalicylate and 1,10-phenanthroline and their crystal structures, Chin. J. Chem. 23 (2005) 1292–1296, https://doi.org/10.1002/cjoc.200591292.
[38] A.B.P. Lever, Inorganic Electronic Spectroscopy, second ed., Elsevier, Amsterdam-Oxford-New York-Tokyo, 1987, p. 863.
[39] Z. Shi, L. Li, S. Niu, J. Jin, Y. Chi, L. Zhang, J. Liu, Y. Xing, A series of d^n transition metal coordination complexes: structures and comparative study of surface electron behaviors (n = 9, 8, 7, 6, 5), Inorg. Chim. Acta. 368 (2011) 101–110, https://doi.org/10.1016/j.ica.2010.12.049.
[40] J.S. Smart, Effective Field Theories of Magnetism, W.B. Saunders Company, Philadelphia, 1966.